Towards Wearable Everyday Body-Frame Tracking using Passive RFIDs

HAOJIAN JIN, Carnegie Mellon University, USA
ZHIJIAN YANG, Tsinghua University, CHINA
SWARUN KUMAR, Carnegie Mellon University, USA
JASON I. HONG, Carnegie Mellon University, USA

We introduce RF-Wear, an accurate and wearable solution to track movements of a user's body using passive RFIDs embedded in their clothing. RF-Wear processes wireless signals reflected off these tags to a compact single-antenna RFID reader in the user's pocket. In doing so, RF-Wear enables a first-of-its-kind body-frame tracking mechanism that is lightweight and convenient for day-to-day use, without relying on external infrastructure. At the heart of RF-Wear is a novel primitive that computes angles between different parts of the user's body using the RFID tags attached to them. RF-Wear achieves this by treating groups of RFID tags as an array of antennas whose orientation can be computed accurately relative to the handheld reader. By computing the orientation of individual body parts, we demonstrate how RF-Wear reconstructs the real-time posture of the user's entire body frame. Our solution overcomes multiple challenges owing to the interactions of wireless signals with the body, the 3-D nature of human joints and the flexibility of fabric on which RFIDs are placed. We implement and evaluate a prototype of RF-Wear on commercial RFID readers and tags and demonstrate its performance in body-frame tracking. Our results reveal a mean error of 8-12° in tracking angles at joints that rotate along one degree-of-freedom, and 21°-azimuth, 8°- elevation for joints supporting two degrees-of-freedom.

CCS Concepts: • **Human-centered computing** → **Gestural input**; **Mobile devices**;

Additional Key Words and Phrases: Smart fabric, wearable computing, RFIDs, gesture-based interfaces, human sensing, antenna arrays, wireless, skeleton tracking

ACM Reference Format:
Haojian Jin, Zhijian Yang, Swarun Kumar, and Jason I. Hong. 2017. Towards Wearable Everyday Body-Frame Tracking using Passive RFIDs. *Proc. ACM Interact. Mob. Wearable Ubiquitous Technol.* 9, 4, Article 1 (September 2017), 23 pages. https://doi.org/0000001.0000001

1 INTRODUCTION

Many of today's wearables can measure the movement of body parts they are attached to. But imagine a wearable system that can track movements of all parts of a user's body as they carry on with their daily activities, all from their handheld device. Such a system could aid in monitoring the health of the elderly without asking them to wear unwieldy equipment. It could also enable more accurate fitness tracking, learning not just the number of steps made by users, but also their gait and step lengths. Further, it could resolve a critical problem faced by today's virtual or augmented reality headsets – the fact that helmets on the head are unaware of the current posture of their users' body or the gestures they make.

Authors' addresses: Haojian Jin, Carnegie Mellon University, 5000 Forbes Ave, Pittsburgh, PA, 15213, USA; Zhijian Yang, Tsinghua University, Beijing, CHINA; Swarun Kumar, Carnegie Mellon University, 5000 Forbes Ave, Pittsburgh, PA, 15213, USA; Jason I. Hong, Carnegie Mellon University, 5000 Forbes Ave, Pittsburgh, PA, 15213, USA.

2474-9567/2017/9-ART1 $15.00
https://doi.org/0000001.0000001

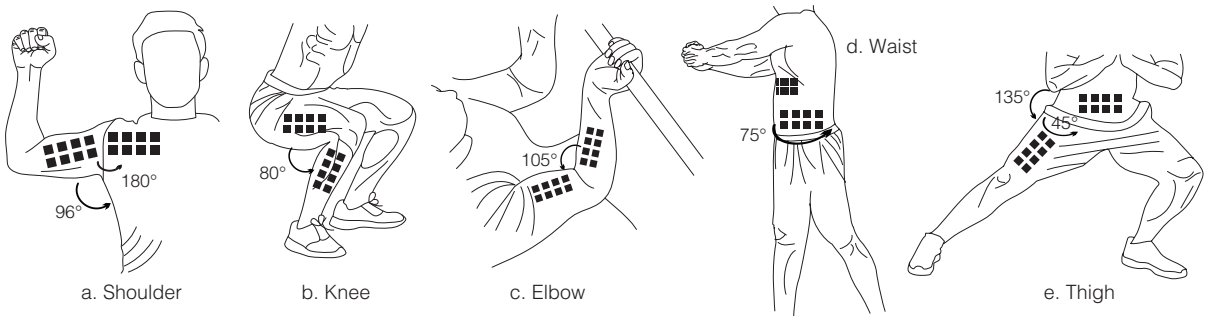

Fig. 1. RF-Wear tracks the user's skeleton using passive RFID tags (annotated as black squares in the figure) that can be woven into the user's clothing. These tags are inexpensive, machine washable and lightweight and are tracked relative to a single portable RFID reader. The figures above illustrate six examples for various joints: shoulder, knee, elbow, waist, and thigh. Our key primitive measures angles between different parts of a user's body by tracking the corresponding RFID tags. RF-Wear then reconstruct the entire body-frame by combining such joint angles.

To deliver all of the above applications and more, one would need to track the entire human body-frame using a solution that is both convenient (meant for everyday use) and ubiquitous (works no matter where you are). While there has been a great deal of past work on tracking the human body, these solutions tend to choose between either being ubiquitous or convenient. For example, infrastructure-based solutions, such as the Microsoft Kinect [51], or LED-based [24] and RF-based solutions [43, 47] can perform accurate body-frame tracking, but operate only in environments where the infrastructure is deployed. In contrast, wearable sensor solutions to track the entire body accurately [3, 15] are portable, yet face impediments for everyday use, be it frequent removal for recharging batteries or prior to machine washing. Indeed, there exists a gap for a ubiquitous body-frame tracking system that is also meant for everyday use.

1.1 RF-Wear : Everyday Wearable Body-Frame Tracking using Passive RFIDs

This paper presents RF-Wear, a first-of-its-kind body-frame tracking solution using low-cost passive RFID tags, each costing a few cents. RF-Wear tracks the user's body-frame using lightweight, machine washable, battery-free ultra-high frequency (UHF) RFID tags [21, 44] that can be woven into the user's clothing [20] (Fig. 1). Such tags can then be tracked and programmed using a single-antenna handheld RFID-reader that can fit into the user's pocket. The RFID reader can be recharged periodically akin to a user's smartphone and may even be integrated directly into future smart-phones [18]. We implement a prototype of RF-Wear on a commercial RFID reader platform and experimentally evaluate its accuracy in tracking parts of the user's body with a motion capture system.

At the heart of RF-Wear's skeleton tracking approach is a simple primitive – measuring angles between different parts of a user's body by tracking the corresponding RFID tags. Essentially, RF-Wear relies on the fact that the skeleton tracking problem can be reduced to tracking angles between various pairs of imaginary lines along the user's body. For instance, a user's posture at the knee when squatting can be measured based on the angle between the lower and upper leg (Fig. 1b).

Yet, tracking RFID tags accurately to compute these angles using a portable handheld device is challenging. State-of-the-art solutions to track RFID tags do so using bulky multi-antenna RFID readers [47]. Such systems measure the angular position of the RFID tags relative to the reader antennas to track their location (Fig. 2a). To measure these angles accurately, they require the antennas on the readers to span several wavelengths (at least a meter or more end-to-end). Naturally, such readers are too bulky to fit in a user's pocket.

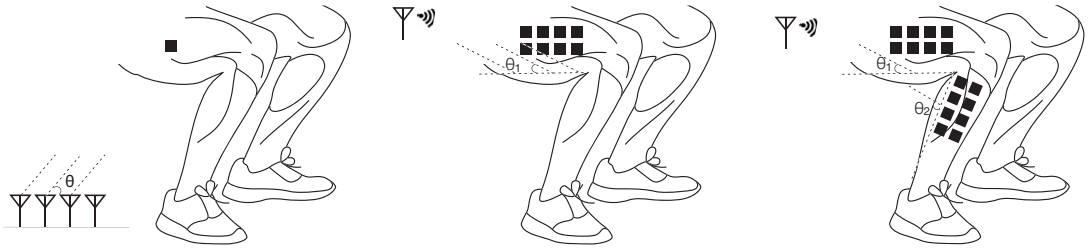

(a) Past work approach (b) Inversed antenna-tag relationship (c) Key primitives

Fig. 2. Our **Key Primitive** infers the orientations of RFID tag arrays relative to the direction of a single-antenna reader antenna by reversing the tag-reader relationship and then measures the relative angle at the joint. In this case, the observed angle (θ_1, θ_2) at the upper and lower leg relative to the reader can be used to infer the angle at the knee joint: $\theta_2 - \theta_1$.

In contrast, RF-Wear enables RFID-based body-frame tracking using a portable single-antenna RFID reader. Our key insight is to employ a multi-antenna array composed of RFID *tags* instead of reader antennas. Specifically, **instead of computing the direction-of-arrival of signals from an individual RFID tag to an array of reader antennas** (Fig. 2a), **we calculate the direction-of-arrival of signals from a single reader antenna to an array of RFID tags** (Fig. 2b). Said differently, this direction-of-arrival is simply the orientation of the array of RFID tags relative to the reader's direction. We show how traditional antenna-array algorithms can be extended to process arrays of RFID tags, as opposed to reader antennas. Figure 2c illustrates RF-Wear's approach in a simplified 2-D context of tracking a user's legs. RF-Wear first measures the orientation θ_1 of the user's thigh relative to an RFID reader using the corresponding array of tags. It then repeats this process at the lower leg to obtain θ_2 and computes the angle at the knee as $\theta_2 - \theta_1$. Observe that RF-Wear's approach does not require the precise location of the RFID reader or indeed mandate that this location be fixed over time. This makes RF-Wear practical to be used with a handheld RFID reader in a user's pocket, whose absolute location is unknown and may change over time.

The rest of this paper describes our solutions to the key challenges in making the above design practical. First, we propose a solution to disambiguate the multiple paths of the signals from the RFID reader to the tags as they reflect off walls, furniture and even the user's own body. Second, we generalize RF-Wear to three-dimensions, allowing for readers that may not be in the same plane as a joint, and joints that may rotate along more than one degree-of-freedom. Finally, we account for the effect of fabric flexibility that may alter the orientation and shape of the RFID array on the user's body.

We implement a prototype of RF-Wear on a commercial Impinj RFID-reader using one single antenna. Our RFID tags cost few cents a piece, are as light and flexible as a scrap of paper, which can be readily embedded in fabric (see Sec. 6). We then attach 2-D rectangular arrays of these RFID tags composed of 6-25 tags, based on available surface area, to fabric placed on different parts of a user's body and track it relative to the RFID reader antenna. Our experiments reveal an absolute error of 8 to 12° in the angle of joints that support one degree of freedom (elbow & knee) and 21° - azimuth, 8° - elevation in the angle at joints that support two degrees of freedom (shoulder). We also present a detailed discussion on the advantages and limitations of our approach.

1.2 Contributions

Our main contribution is a novel solution that enables a wearable, accurate and light-weight body-frame tracking using passive low-cost RFIDs attached to the user's clothing. RF-Wear achieves this using a handheld RFID reader in the user's pocket whose location or movement does not need to be calibrated.

Our specific contributions are as follows:

- A novel algorithm that infers the orientation in 3-D of an array of RFID tags relative to the direction of a single-antenna reader antenna by reversing the tag-reader relationship.
- A mobile RFID sensing primitive that can measure the one degree-of-freedom joint angle using two 2-D RFID arrays, even if the only RFID antenna position is unknown and non-static. Our approach accounts for the multiplicity of RF signal paths from the RFID tags to the reader and avoids the error-prone triangulations.
- A practical body-worn RFID tags placement solution considers the unique constraints of the human body and fabric movements: the multiple degrees of freedom of human joints, the limited flat surface area, and the flexibility of fabric.
- A detailed prototype implementation and evaluation of RF-Wear, including different RFID-array configurations demonstrates high accuracy in tracking joints that support different degrees of freedom.

2 RELATED WORK

Past work in the body tracking and gesture sensing space falls under two broad categories: infrastructure-based systems and wearable systems. The prior work on wearable systems can be further classified by if the system is suitable for daily use.

	Infrastructure-based	Wearable	
		Not Suitable for Daily Use	Suitable for Daily Use
Gesture Sensing	[9, 22, 23, 27, 31, 34, 43]	[5, 14, 50]	[33]
Body Tracking	[2, 4, 24, 26, 32]	[8, 10]	RF-Wear

2.1 Infrastructure-based systems

Vision and RF-based Infrastructure: There has been much past work on gesture sensing/body tracking using stationary sensors (e.g. cameras) in the environment. Microsoft Kinect [51] is one of the most successful innovations that performs full-body skeleton tracking using depth cameras [25]. The leap motion controller [26] is another popular input device for hand gesture sensing with declared sub-millimeter accuracy. Beyond cameras, recent work has also demonstrated the use of ambient LED lights to track postures of the upper body [24]. RF-based systems have sought to employ multi-antenna radio receivers to classify gestures and track users through-walls using radio-signals [2, 34]. Unlike RF-Wear, these systems can only monitor the user's gestures in the specific environments where the required infrastructure is deployed and calibrated.

RFID-based Infrastructure: There also has been much interest in the use of multi-antenna RFID arrays for fine-grained positioning and gesture monitoring [43]. Unlike the traditional signal strength based schemes [28], recent systems [43, 48] locate the RFID tags based on the low-level phase information of backscattered radio waves and achieve cm-level accuracy. However, these systems often require a large reader antenna array to position the tags through triangulation or tri-lateration [43, 48]. Such multi-antenna readers are too bulky to be used as handheld systems.

Recent work has also investigated the use of single RFID antenna for a variety of coarse-grained sensing tasks, such as discrete gesture classification [9, 22, 23, 39], exercise monitoring [9] and object-recognition [23]. These systems are designed to classify between a few coarse positions that the RFID tag may be in, and do not provide their fine-grained locations or orientations as a function of time. RF-Wear builds on such systems to provide a novel solution that can accurately track the continuous angle between different parts of a user's body, using a compact single-antenna RFID reader.

2.2 Wearable Systems

Wearable Body Tracking: The most straightforward approach to implement wearable body tracking is deploying the sensors on the body/clothes directly. Early research in gesture tracking deployed digital angle measures at the user's joints to track posture [7, 38]. One of the first textile-based wearable systems was the sensor jacket [10], which measured the wearer's upper body posture utilizing eleven knitted stretch sensors placed over the joints. A more sophisticated example is SensorTape [8], which deploys a dense light-weight inertial sensor network on tapes to track the tape curvature.

Such systems are often designed to be used in specific contexts where the added bulk and cost are not pertinent, e.g. therapy, sports training, and 3-D movie making. Another key challenge with these systems is that they require batteries and electronics in clothing which add to bulkiness and are not machine washable. They are not intended for day-to-day use beyond these contexts. In contrast, RF-Wear designs a system that is inexpensive, non-intrusive and light-weight when attached to fabric, without compromising on tracking accuracy.

Smart Fabrics for Daily Use: Designing non-intrusive fashion and aesthetic smart fabrics is an emerging topic [12, 33, 49]. Project Jacquard [33] uses conductive yarns to weave the touch and gesture-sensitive areas on the textile in a non-intrusive way. Biologic [49] takes advantage of the hygromorphic phenomenon in living cells to build electronics-free fabric material. While these material science breakthroughs are promising, their sensing capability is restricted to specific types of inputs – touch and humidity, respectively.

The wireless and battery-free nature of passive RFID tags make them an ideal candidate for non-intrusive smart fabrics [21]. However, existing applications are still limited to use the unique IDs for identifying different parts of the body/objects grasped [20, 27, 31, 44] or classifying a few discrete gestures [22].

RF-Wear strives to build a system that is suitable for daily use when embedded in fabric without compromising on fine-grained body-tracking accuracy. Further, unlike inertial systems that rely on movement (angular velocity and/or acceleration), RF-Wear achieves reliable and accurate posture monitoring of both static and mobile body parts. It achieves this using battery-free and machine washable RFID tags [19, 45] embedded in the user's clothing.

3 BACKGROUND

Passive RFID tags communicate with the reader antenna by harvesting and reflecting (i.e., back-scattering) energy from the radio wave transmitted by the reader antenna. Figure 3 illustrates a conceptual diagram of backscatter communication. Each RFID tag has a small Electronic Product Code (EPC) memory to hold no more than 2KB of data. The low-cost tag used in RF-Wear has a more limited memory and contains only a 96-bit or 128-bit serial number. The tag modulates backscatter signals using ON-OFF keying by changing the impedance on its antenna. The reader can then recognize different tags by demodulating this signal.

The role of RF phase in backscatter-based localization: Recent COTS RFID readers support fine-grained resolution in detecting the phase of received RF signals with accuracy ≈ 0.0015 radians [48]. This accuracy offers an opportunity to locate the object within millimeter-level displacement. Figure 3 (left) depicts the details of the process. Suppose d is the distance between the reader antenna and the tag, the signal traverses a total distance of $2d$ back and forth in backscatter communication along line-of-sight. Besides the RF phase rotation over distance, the reader's transmitter, the tag's reflection characteristics, and the reader's receiver circuits will all introduce additional phase rotation, denoted as θ_T , θ_{Tag} and θ_R respectively. The reader antenna will therefore report a phase difference ($\Delta\theta$) of transmitted (θ_1) and received signal (θ_2), given by:

$$\Delta\theta = \theta_2 - \theta_1 = (\frac{2d}{\lambda} * 2\pi + \theta_T + \theta_{Tag} + \theta_R) \; mod \; 2\pi; \; \lambda = \frac{c}{f}; \tag{1}$$

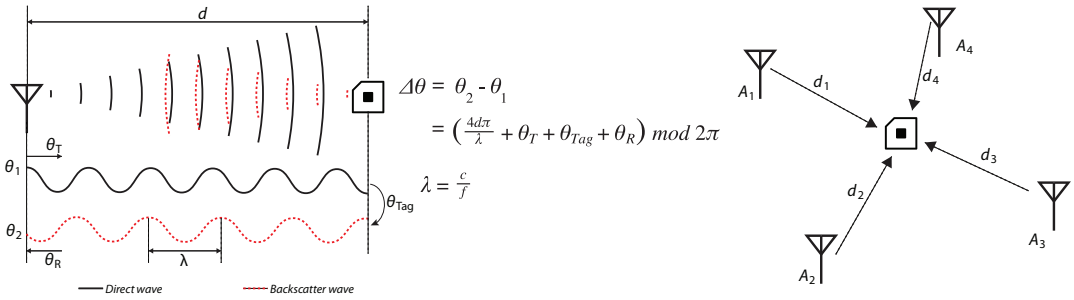

Fig. 3. Background. (Left) Different types of RF phase shifts in backscatter communication. (Right) Using the antennas at known positions to infer the tag position.

where λ is the wavelength of radio signal at frequency f and c is the speed of the light. Various factors can impact the θ_T, θ_{Tag} and θ_R. For example, the thermal noise from the reader receiver can introduce a mean measurement error of 0.1 radians [48]. The phase values measured at a given position can vary significantly across different tags (0.30 $\sim$ 5.84 radians) [48] and orientations (0 $\sim$ 2π radians) [46]. All these errors will impact the ranging accuracy and cannot be ignored in practice. We will discuss how we address these challenges in Sec 4.1.

Using known reader antenna positions to locate the tag: Past systems on locating RFID tags have relied on bulky multi-antenna RFID readers and require a priori knowledge of the position of the reader antennas [43, 48]. Figure 3 (right) illustrates positioning in the context of a 4-element RFID reader antenna array. These systems rely on the fact that the reflected signal from a given RFID is received with slightly different phase shifts, across multiple spatially-separated reader antennas, depending on the tag position. If the reader antennas' positions are known, we can construct a likelihood heatmap (i.e., an RF hologram [43]) of tag location using the phase observations. However, the reader cannot retrieve the absolute distance directly from the phase due to the *mod* operation in Eqn. 1. To resolve this ambiguity, these systems require multiple antennas at various known locations [43, 47, 48] and a well-defined and known spacing distance between antennas. Indeed, the more antennas in the system, the greater the resolution in the measured tag location.

4 AN OVERVIEW OF RF-WEAR

In this section, we provide a brief overview of RF-Wear's approach. RF-Wear's key primitive is a mechanism that computes the angles between different parts of the user's body. RF-Wear then combines angle measurements across various joints in the body (hip, shoulder, elbow, knees, etc.) to track a person's body frame.

To compute these angles, RF-Wear relies on passive RFID tags embedded within the user's clothing covering the surrounding parts of the body. These RFID tags cost few cents a piece, are about the size of a U.S. quarter and are as light and flexible as a scrap of paper. This means that RFID tags can be seamlessly stitched into layers of fabric [13, 20, 21]. RF-Wear works with any arbitrary number of tags (>4) embedded on each part of the user's clothing, depending on the available surface area.[1] In general, the more tags available on a body part, the more accurate RF-Wear will be.

Before running RF-Wear's algorithms, we assume that the RFID reader is aware of the initial configuration of the RFID tags on clothing, i.e. which tag is on shoulder/left leg/right upper arm, etc. The manufacturer can either store the layout information in EPC memory of each tag or maintain an online database, where one can lookup the layout given the unique IDs of tags. However, we do not assume that the absolute position of the reader

[1]Our results in Sec. 7.1 discuss system accuracy versus the number and geometry of RFID tags, per body-part.

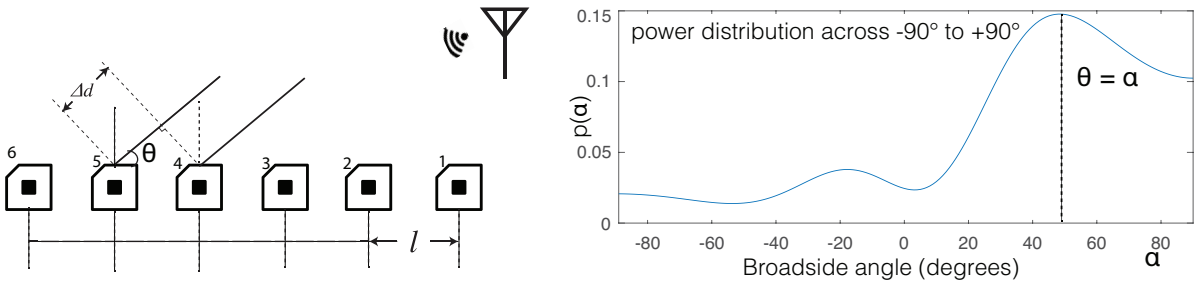

Fig. 4. **RF-Wear in 2-D**: (Left) measures the angle-of-arrival θ from the reader to a linear array of tags. (Right) depicts $P(\alpha)$ the relative power of the received signal along different angles-of-arrival α. Note a maximum at exactly $\alpha = \theta$.

antenna is known or even constant over time. In other words, our system is designed to accommodate a moving reader antenna whose absolute location may change over time, as the user carries on with his/her daily activities.

Using a compact RFID reader in the user's pocket to perform body-frame tracking has three important implications. First, we can at most use a single reader that is compact and at best supports a single-antenna, meaning that one cannot leverage the rich literature on multi-reader-antenna arrays for tracking body-worn tags. Second, RF-Wear must account for the fact that the position of the reader itself is dynamic and unknown, owing to the fact that the reader will move alongside the user within his/her pocket. Finally, signals from the tags to the reader are likely to traverse along multiple paths as they reflect off walls, furniture and the user's body. This introduces errors in determining the true angle-of-arrival of the signal from the passive tag to the reader antenna. The rest of this section describes RF-Wear's approach in dealing with the above challenges. For simplicity, our discussion starts in a 2-D space and we will discuss the important challenges pertaining to extending RF-Wear to 3-D in Section 5.

4.1 Computing the orientation of an array of RFID tags from a single-antenna reader

RF-Wear's key approach in tracking the orientation of a part of the user's body using a handheld, single-antenna reader relies on inverting the relationship between reader antennas and the tags in antenna-array literature. Instead of tracking an individual RFID tag from multiple RFID reader antennas at known positions, we infer the direction of the incoming signal from the antenna to multiple passive RFID tags in a known geometry. While deploying widely-separated RFID antennas is bulky and expensive, our approach is cheap and simple, only requiring to attach multiple passive RFID tags to the user clothing in a pre-defined geometry.

Our approach is best explained with an example. Figure 4 (left) illustrates in free space and 2-D, a simple uniform linear array of RFID tags with incoming signals from the single-antenna reader at an angle θ. In this example, the distances (aperture) l between any two adjacent tags are consistent across the linear array and known as a priori. If we can infer the difference in time of arrival of the signals at tag 4 and tag 5, we can compute the difference in the distances they traverse, Δd. Based on Δd and l, we can then calculate the direction-of-arrival (θ) of the incoming signal from the antenna to the uniform linear array. Indeed, it is easy to see that: $\Delta d = l \cos\theta$. This direction-of-arrival (θ) defines the orientation of the RFID-array in 2-D space, the quantity we seek to obtain.

To compute Δd and therefore θ from phase rotations, we rely on the phase of the wireless channels measured at any two adjacent tags. Recall from Eqn. 1 that Δd depends on the phase measurement of the tags. Yet, this phase value also depends on additional phase rotations that we do not care about and introduce error: θ_T, θ_{Tag} and θ_R from the reader's transmit chain, the tag and the reader's receive chain respectively. One must therefore eliminate these errors to compute Δd accurately.

Our approach to overcome this challenge relies on the relative phase between pairs of adjacent RFID tags. Given that we deal in the difference in phase between two tags, any phase offset from the RFID reader, i.e. θ_T and θ_R disappear. More interestingly, we observe empirically that for RFID tags from the same manufacturer, the quantity θ_{Tag} is also identical and cancels out, provided the tags are oriented towards the same direction in space (see results in Sec. 7.1). Indeed, one can ensure this at the time of manufacture by orienting all RFID tags in the same direction on a given plane. An important exception to this property is the effect of fabric flexibility in 3-D space, when tags may be oriented towards slightly different directions when fabric crumples, a challenge we deal with in Sec. 5.3.

To illustrate our solution mathematically, let θ_4 and θ_5 be the raw phase observations of the backscatter radio from tag 4 and tag 5, respectively in Fig. 4. Then, it is easy to see that θ can be obtained as:

$$cos\theta = \frac{\Delta d}{l} = \frac{\lambda(\theta_5 - \theta_4)}{4\pi l} \tag{2}$$

Note that we divide by 4π as opposed to 2π as in Eqn. 1 because the radio signal travels twice the distance – forwards and backwards in backscatter communication.

Multiplicity of Signal Paths: Our discussion thus far assumes that the signals from the reader to the tag array traverses along a single path. In practice, however, signals traverse multiple paths as they bounce of objects in the environment (e.g. the walls, furniture or the user's body). RF-Wear resolves this by applying the MUltiple SIgnal Classification (MUSIC) [36] algorithm on an array of RFID tags, as opposed to RF-antennas. At a high level, the MUSIC algorithm uses an eigen sub-space decomposition approach to separate signal paths along different spatial angles. Mathematically, $\mathbf{h} = [h_1, \ldots, h_n]$ represent the wireless channels from the n RFID tags to the RFID reader, where each tag is separated by a distance l. The absolute value square of these channels denotes received signal power from the tags and the angle denotes the incoming signal phase. Then we can write the normalized power (a probability metric) of the received signal $P(\alpha)$, along any arbitrary incident angle at the array α as:

$$P(\alpha) = \frac{1}{|a(\alpha)E_N E_N^* a(\alpha)^*|}, \text{where: } a(\alpha) = [e^{4\pi j r_i cos(\alpha)/\lambda}]_{i=1,\ldots,N} \tag{3}$$

where r_i denotes the distance between the corresponding tag to the center of the tag array, E_N is a matrix of the noise-eigen vectors of hh^*, $(.)^*$ is the conjugate transpose operator.

Figure 4 (right) depicts an example of the relative power of the received signal along different angles-of-arrival α. Note a distinctive peak at the angle (θ), the spatial angle-of-arrival of the signal from the reader to the tag array. Even in the presence of reflectors, the strongest peak of $P(\alpha)$ occurs typically at θ, with other paths producing smaller peaks. We deal with the ambiguity that results when $P(\alpha)$ contains multiple dominant peaks in Sec. 4.3.

Array Geometry: We observe that Eqn. 3 while illustrated on a linear array of tags, readily generalizes to arrays of different geometries [11]. However, we do require two important constraints on array geometry. First, the geometry of the array (i.e. the spacings: r_i's) must be a known priori, for instance at the time the fabric is manufactured. Second, we limit the spacing between adjacent tags in the array. To see why, observe that for the Eqn. 2 to result in valid and unique values of θ (with $|\cos\theta| \leq 1$), we require the spacing between adjacent tags to be smaller than a quarter of the wavelength ($l \leq \lambda/4$). This provides an important geometric constraint in how we place RFID tags on fabric – adjacent tags should be no more than $\lambda/4$ away. Our results in Sec. 7.1 study the accuracy and performance of RF-Wear tag arrays in different geometries.

4.2 Dealing with a "moving reader in the pocket"

Given the orientation of different parts of the body relative to the RFID reader, RF-Wear needs to compute the angles of different joints. The key challenge in doing so is the fact that the RFID reader itself is at an unknown

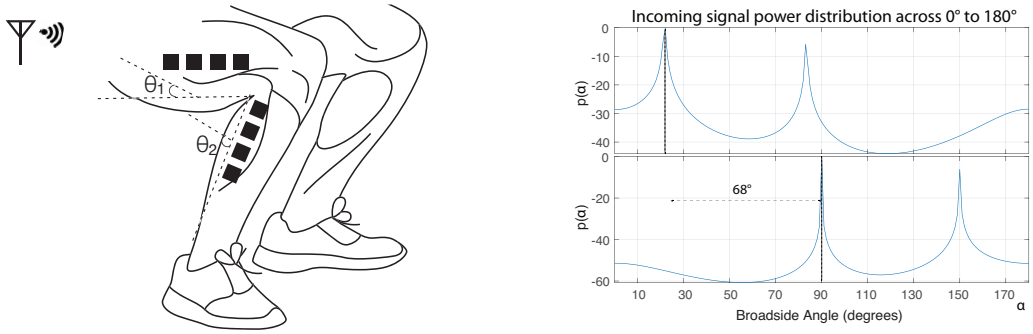

Fig. 5. **Computing angle at the joint in 2-D**. (Left) Given the angle-of-arrival at two arrays θ_1 and θ_2, the interior angle of the joint is $\theta_2 - \theta_1$. (Right) $\theta_2 - \theta_1$ can be computed as the shift in MUSIC spatial spectrum $P(\alpha)$ between the two arrays.

location in the user's pocket. To make matters worse, the location of the reader can change over time as the user moves.

RF-Wear can obtain the angles of different joints in the body without knowing the current location of the RFID reader. At a high level, our approach relies on the fact that the angle of a given joint is simply the relative orientation of the two adjacent body parts with respect to the reader. Figure. 5 (left) illustrates this principle in the context of orientations θ_1 and θ_2 of the thigh and lower leg relative to the in-pocket RFID reader. It is easy to see that the angle at the knee is $\theta_2 - \theta_1$ as shown. We note that the above approach assumes that the position of the RFID reader has not moved significantly over the time period of collecting wireless channel measurements from the RFID tags on the body. In practice, commercial readers can query RFID tags at the rate of up to 40 Hz which makes doing so achievable given the reader moves at human speeds.

4.3 Mitigating ambiguity from signal multipath

Finally, we note that our discussion so far has assumed that signals from the reader to the tag array arrives along a single dominant direct path. In practice, obstacles between the reader and the tags such as the body itself could weaken the direct path, resulting in multiple dominant signal paths. This results in an array of possible angles that are likely to be the orientation of the reader. Mathematically, this manifests as multiple local maxima of $P(\alpha)$ leading to ambiguity on the true orientation of the array.

RF-Wear addresses this challenge by exploiting the structure of multipath. Specifically, recall from the laws of reflection that one can think of multiple signal paths as signals from "virtual sources" that are mirror images of the RFID reader along various reflecting surfaces. Many of these surfaces, e.g. walls, furniture and large areas of the body are likely to be shared across adjacent body parts across from a joint. Further, recall from our discussion in Sec. 4.2 above that for each such virtual source, their angle-of-arrival θ_1 and θ_2 relative to two joints would differ exactly by the angle at the joint $\gamma = \theta_2 - \theta_1$. Said differently, for each virtual source, one would see two local maxima of $P(\alpha)$ across the two body parts that differ exactly by γ (see Fig. 5). Indeed, if all reflectors are quasi-static and shared across the two body-parts, $P(\alpha)$ of one body-part would simply be an γ-rotated version of the other. Consequently, RF-Wear can retrieve γ by simply performing a cross-correlation of the two $P(\alpha)$ distributions to compute the relative shift. We note that in practice, there could be smaller reflectors (typically, small parts of the body) that may be dominant influence on the signal for one body-part, but not the other, leading to noise in our cross-correlation. Our results reveal that in practice, there are a sufficient number of dominant reflectors shared by adjacent body-parts to guarantee high accuracy in joint angle-tracking (see Sec. 7).

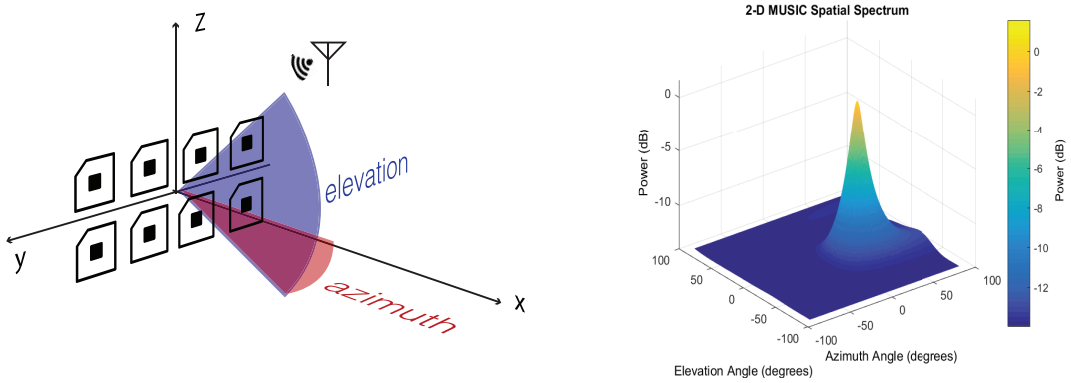

Fig. 6. **RF-Wear in 3-D**: (Left) depicts the definition of the polar and azimuthal angle-of-arrival (ϕ, ψ) from the reader to a rectangular array of tags. (Right) Depicts $P(\phi, \psi)$ the power of the received signal along different angles-of-arrival (ϕ, ψ).

5 RF-WEAR SYSTEM DESIGN IN 3-D

Our discussion thus far has been constrained to two-dimensions. However, generalizing our approach to 3D elicits three important challenges. First, how does our system deal with an RFID reader that may not be in the same plane as the joint? Second, what if the joint itself rotates along more than one-degree of freedom? Finally, given that tags are attached to flexible fabric, what if it folds and crumples, distorting the geometry of the array, crucial to our analysis? The following sections address these concerns.

5.1 Tracking joints that rotate along one degree-of-freedom in 3D space

In this section, we discuss how RF-Wear can be extended to track the angles of joints in 3D. To begin with, let us consider joints that rotate along one degree-of-freedom. A key implication of operating in three-dimensional space for such joints is that the RFID reader antenna may not be in the same plane as the joint itself. Indeed, in practice, this is extremely difficult to ensure, given that the location of the reader in the user's pocket is likely to change over time. To see why this is the problem, recall our approach from Figure 5, which subtracts the angle between the two tag-arrays $\theta_2 - \theta_1$ to compute the relative angle of the joint. Clearly, should the RFID reader move slightly so as to rotate about the lower leg, θ_2 would remain unaffected, while θ_1 would change. Indeed, it is possible for $\theta_2 - \theta_1$ to vary arbitrarily as the RFID reader moves off-plane, even if the angle of the joint remains exactly the same.

RF-Wear overcomes this ambiguity by using 2D RFID arrays. Specifically, it relies on rectangular arrays of RFID tags that can decouple the incoming direction-of-arrival of the reader into azimuth and elevation. Figure 6 (left) illustrates a simple example of such a rectangular RFID array. For such a rectangular array, we define the long side as the y axis and the short side as the z axis. We can describe any direction of the incoming signal using a combination of azimuth (ϕ_1) and elevation (ϕ_2). Azimuth is a polar angle in the x-y plane, with positive angles indicating counterclockwise rotation of the origin point; elevation is the angle above (positive angle) or below (negative angle) the x-y plane. Similar as the 2D example depicted in Figure 4, we can compute the relative power of the received signal along different angles-of-arrival:

$$P(\phi, \psi) = \frac{1}{|a(\phi, \psi) E_N E_N^* a(\phi, \psi)^*|}, \text{ where: } a(\phi, \psi) = [e^{4\pi j r_i cos(\phi) sin(\psi)/\lambda}]_{i=1,\ldots,N} \quad (4)$$

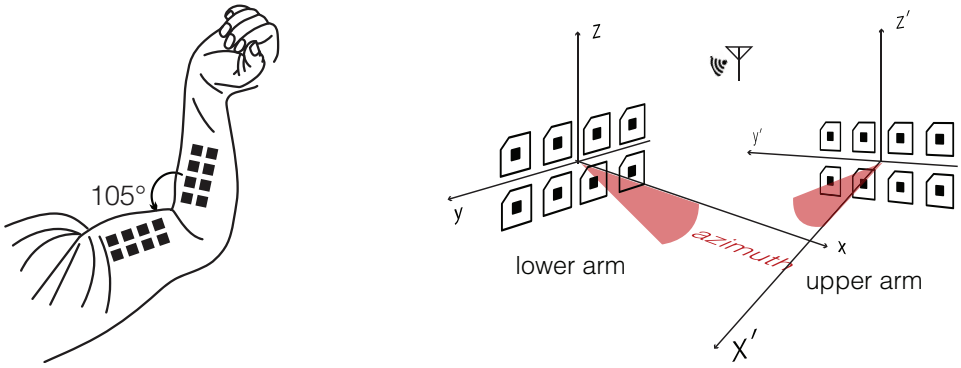

Fig. 7. **Computing the angle at the elbow joint in 3D:** Demonstrates our approach in calculating the angle at the intersection of body parts (upper and lower arm) for joints rotating in 3D using a rectangular array of RFID tags.

where r_i denotes the distance between the corresponding tag to the center of the tag array. Fig. 6 (right) depicts the power of received signal along different azimuth and elevation angles.

Figure 7 further illustrates an example of 1DOF tracking primitive on the elbow joint. Two tag arrays are attached to the lower arm and the upper arm respectively, sharing the same z axis. We can use Eqn. 4 to infer the azimuth and elevation angle of the two RFID arrays. Assuming $P(\phi, \psi)$ would be maximum at exactly (ϕ_1, ψ_1) and (ϕ_2, ψ_2) for the two RFID arrays, the elbow joint angle then can be computed as $\phi_2 - \phi_1$, the difference of two azimuth angles (Fig. 7 right). Note that as before, we can mitigate multipath by computing the cross-correlation of $P(\phi, \psi)$ to find the difference in azimuth (see Sec. 4.3). Our approach can readily be applied to various joints that rotate along one-degree of freedom on the human body, e.g. knees and elbows.

5.2 Tracking joints that rotate along two degrees-of-freedom

The above approach can readily be generalized to also compute angles at joints that rotate along two degrees of freedom, such as the ball-and-socket joint in the shoulder. Given that such joints do not rotate on any given plane, one cannot characterize the relative angle between the two body parts in terms of one angle in 3-D space. To illustrate, Figure 1(a) depicts the relative orientation of the upper arm and torso in three-dimensions in terms of two angles: their relative azimuthal angle α along the plane of the torso and the polar angle β that captures the elevation of the arm relative to the torso off-plane.

RF-Wear computes these two angles as the difference in azimuthal angles $\phi_2 - \phi_1$ and polar angles $\psi_2 - \psi_1$, respectively, of the two joints. Indeed, for any rotations along one degree-of-freedom along the plane of the torso, this angle reduces to the difference in azimuthal angles, $\phi_2 - \phi_1$ as described above. Similarly, for rotations at a given relative azimuth, the upper arm would rotate on the plane perpendicular to the torso, while the torso remains static; meaning that $\psi_2 - \psi_1$ would capture their relative out-of-torso-plane angle. Indeed, it is easy to see that these two rotations are independent allowing us to fully characterize rotations of the two-degree of freedom joint as $\phi_2 - \phi_1$ and $\psi_2 - \psi_1$. More precisely, we compute these differences by accounting for multipath ambiguity by performing a cross-correlation of $P(\phi, \psi)$ per array, both along azimuth and polar axes and then computing the difference across arrays (Sec. 4.3).

Yet, visualizing these angles in 3-D space requires overcoming two important limitations. First, we note that the angle differences $\phi_2 - \phi_1$ and $\psi_2 - \psi_1$ are defined in a coordinate system relative to the direction of the reader antenna. Re-orienting this coordinate system to a meaningful 3-D coordinate system requires the location of the reader antenna. Our approach to overcome this challenge triangulates the reader antenna using *multiple*

RFID tag arrays on the body, at known relative locations. We first pose this as an optimization problem with the wireless channels, as well as their relative location as known quantities, while the location of the reader antenna is unknown. This is a maximum likelihood problem analogous to [48] with a key difference – the role of reader antennas and RFID tags inverted. We then solve this optimization problem using a stochastic gradient descent algorithm with multiple randomly chosen initial estimates of the reader location [48]. Once the reader location is known, we translate (ϕ, ψ) coordinates to the coordinate system of the body. More precisely, we compute the coordinate transform of the family of (ϕ, ψ) coordinates in $P(\phi, \psi)$ to account for multipath ambiguity (alg. 1). We can then compute relative angle differences as before.

Algorithm 1 Applying coordinate transform to direction-of-arrival profiles $P(\phi, \psi)$

Input: Original spectrum $P(\phi, \psi)$, Transformation matrix R
Define: $f(\phi, \psi)$: Function correlating orientation to corresponding directional vector
Output: New spectrum $P'(\phi', \psi')$
for Each point in spectrum P **do**
  $\phi', \psi' = f^{-1}(Rf(\phi, \psi))$
  $P'(\phi', \psi') = P(\phi, \psi)d\phi d\psi / (d\phi' d\psi')$
end for
return $P'(\phi', \psi')$

A second important challenge is that unlike the azimuthal angle, the polar angle cannot distinguish between off-plane angles that are "upwards" and "downwards" owing to the symmetry of these two scenarios for an RFID array along a given plane. This means that our body-frame tracking angles off-plane always have an ambiguity of $\pm 90^\circ$. RF-Wear can resolve this ambiguity by mounting a secondary RFID array on one body part (e.g. along the side of the torso for the shoulder joint) that is orthogonal to the other array. This would provide a secondary source of information, where the roles of azimuthal and polar angles are flipped, thereby helping to resolve ambiguity.

One might wonder how RF-Wear can generalize to support joints that may rotate along all three-degrees-of freedom (e.g. the wrist). One approach to achieve this is to mount additional arrays along three mutually orthogonal axes at every joint. However, doing so on smart fabric would neither be convenient nor aesthetically appealing. Our approach is therefore limited to joints that rotate along at most two-degrees of freedom – in other words all joints on the body barring the wrist and ankle. In addition, our approach does not apply to smaller joints at extremities whose surface area is insufficient and attaching RFID tags would be unwieldy (i.e., the fingers and toes). We discuss these limitations in Sec. 8.

5.3 Dealing with Fabric Flexibility

To operate with high accuracy, RF-Wear must account for the flexibility of fabric that is likely to change the geometry of RFID tag arrays. Specifically, recall that RF-Wear's algorithms for body-frame tracking assume that the structure of the array whether linear or rectangular remains rigid and flat on a surface over time. In practice however, fabric flexibility is likely to change both the relative distance and orientation of the tags over time, introducing errors to measurement. Of course, different types of fabric offer different degrees of flexibility, and consequently, different levels of accumulated error.

Our solution to deal with this problem seeks to fold in mathematical models of flexible fabric [16, 35] into our RFID array processing equations to minimize this error. Specifically, we rely on a few salient features of fabric folding [35]. First, the expected change in distance between any two tags for most fabric is limited to a

few centimeters. More crucially, tags are on average expected to move closer to each other, rather than further away given that folding is more common than fabric stretching. Next, the folds generated in fabric are likely to remain even as the user moves their joints. Finally, the relative ordering of tags, already separated by several centimeters, is unlikely to change due to fabric flexibility.

RF-Wear therefore reformulates the MUSIC algorithm taking into account the expected scaling factor μ in relative distances between array elements (i.e. RFID tags). It measures a pre-programmed expected scaling factor of the distance between pairs of RFID-tags taking into account the flexibility of fabric. These standard deviations are experimentally derived and programmed into RFID tags at the time of manufacture, so that they can provide this information to the reader when queried. To illustrate the mathematical generalization for the case of the 2-D linear array of RFID tags (Eqn. 3), we can re-write $P(\alpha)$ as:

$$P(\alpha) = \frac{1}{|a(\alpha)E_N E_N^* a(\alpha)^*|}, \text{ where: } a(\alpha) = [e^{4\pi j r_i \mu cos(\alpha)/\lambda}]_{i=1,\ldots,N} \tag{5}$$

Where l_i, E_N, j, λ and N are defined as in Sec. 4.1. We make a few important observations about our fabric flexibility approximation as described below:

- **Distances between tags**: we note that the above expression estimates the orientation of the RFID array taking into account an average-case estimate of the separation between tags. In practice though, the shift between tags may vary about the mean introducing errors to our estimate in orientation. However, recall that our interest is in the angle of a joint which is the *difference* in orientation of two body parts. Given that fabric flexibility is likely to introduce similar quantum-of-error in the orientation of the two parts, RF-Wear benefits from much of this error canceling out.
- **Individual tag orientation**: We notice that the phase values can change significantly if the tag orientation changes leading to measurement errors as discussed in Sec. 4. In practice, the tag orientation changes are typically less than <10°, which introduce a tolerable phase observation noise. Moreover, algorithms such as MUSIC rely largely on the phase differences of multiple pairs of tags, which further de-noises our measurements. Finally, we choose commercial RFID tags from among 20 different types that interact best with the human body and whose phase varies minimally across orientations (see Sec. 6).
- **Fabric material**: The quantum-of-error due to fabric flexibility largely depends on the nature of fabric used. Our experiments in Sec. 7 compute the value of μ through a one-time-process per fabric used. We present our results for three different types of fabric in our experiments in Sec. 7.2.

6 IMPLEMENTATION

RFID Tags: We implement our prototype by attaching paper-thin commodity passive RFID tags to regular clothes, including cotton pants, a sweater and a jacket (Fig. 8). Searching for the ideal RFID tags for RF-Wear is a non-trivial task. First, the human body attenuates radio signals. Although the tags will be attached to the fabric, ideal RFID tags should have a consistent performance on/off the body. Second, radio sensitivity and directivity are important aspects to consider. If the RFID tag has a strong directivity, the tags can be seldom detected if they do not directly face the reader antenna. Third, ideal RFID tags should have a small and flexible form factor, which can be embedded into the clothes in a non-intrusive way. Our implementation uses the OmniID IQ 150 tags after a careful comparison of 20 different types of RFID tags to minimize the effect of RFID tag orientation (a partial list is in Table 1).

RFID Reader: While there are several commercial handheld single-antenna RFID readers on the market [1, 29, 42] (up to 12 hours battery life), none of them provide the necessary open software interface (API) to provide wireless channel state information (magnitude and phase). We, therefore, chose the Impinj Speedway RFID reader equipped with a single Ettus VERT900 antenna (Fig. 8), which provides the necessary software interface for wireless channels.

Fig. 8. **RF-Wear prototype on body**. We implement RF-Wear on OmniID IQ 150 tags attached to clothing and an Impinj Speedway RFID reader connected to a single-antenna. The tags are attached to fabrics of different material (a sweater is shown here) and on different body parts (around the knee, elbow, shoulder) the angles of these joints are tracked.

Table 1. A partial list of RFID tags characteristics

UHF RFID Model	Size (cm)	Flexible	Refresh rate (Hz) in the air/on the body (1m away)
Xerafy MicroX	5.1 x 3.63	X	23.8/31.8
Alien Square ALN-9629	2.55x2.55	✓	28.4/0
Alien Squiggle ALN-9740	9.82 x 1.23	✓	30.2/0
Confidex Silverline Blade	6.0 x 2.5	✓	25.2/28.3
OMNI-ID IQ 150	5.2 x 1.25	✓	28.1/24.4

Note that while this reader supports four antennas, we disabled three of its antennas and connected only a single-antenna (with corresponding FCC power limits). Our prototype system is therefore designed to operate in the same power-regime as commercially-available handheld RFID readers.

Software: To comply with FCC regulation, RFID readers (in the USA) "frequency hop" across 50 channels from 902 MHz to 928 MHz at an interval of approximately 0.2 seconds. Once the RFID tags are in the operation range, the reader will produce an observation stream that contains all the low-level wireless channel information, including RFID UUID, phase, signal strength, frequency, etc.

RF-Wear uses a sliding window technique to extract the quasi-simultaneous readings for different tags from the data stream. First, we only extract the tag readings at the same frequency. Second, all the tag readings need to occur in a time span of 0.1 seconds. Third, when the 0.1-second duration expired, RF-Wear will execute based on the partial observations. In practice, some of the tags may become invisible due to the potential body occlusion. Our algorithms can then run on the partial sensor array data with a sacrification of accuracy.

Finally, we infer the joint angle based on the two sequential readings from the corresponding tag arrays and feed this joint angle to a Kalman filter.

Real-Time Performance: In our experiments, this sliding window technique can generate around 30 independent tag array readings per second for each tag array. Partial measurements are observed rarely, particularly when the tag array at extreme angles. We implement the system in python in real-time. The most computing intensive step is computing the spectrum profile, which takes around 0.015s to process one tag array.

Our sensing pipeline is faster than the prior state of the art: IDSense (2s) [22] and RapID (200ms) [39]. The key difference is that we run predictions based on each independent tag reading, while [22, 39] collect the sequential

readings in a time duration to counter the noisy measurements. Our approach de-noises implicitly through the tag redundancy and prior tag array layout knowledge.

7 EVALUATION

We present a detailed experimental evaluation to understand the performance and limitations of RF-Wear. Our evaluation is organized as follows.

1.*Array configuration*: Different geometric configurations of a 2-D tag array in estimating the orientation.
2. *Fabric flexibility*: Different fabric materials in estimating the orientation of each RFID array.
3. *Motion capture evaluation*: Tracking the performance of an on-body deployment at elbow, knee, shoulder.

Metric: To characterize RF-Wear's performance, we mainly focus on angular error at the joint *i.e.*, the deviation of estimated angle from the ground truth.

7.1 Array Configuration

During our evaluation, we find that increasing the number of tags and the aperture can both improve the accuracy. However, the available flat surface areas of different body parts are limited. Moreover, squeezing the antennas too close can be counter-productive owing to the effects of fabric flexibility. To understand these trade-offs, we conduct experiments with different array configurations.

Method: We perform this off-body experiment with the Alien Square ALN-9629 RFID tags mounted on a rigid wooden platform (Fig. 9) at different spacings that can be accurately measured. We choose these square tags because the square shape allows us to experiment various distances between adjacent tags systematically and uniformly along both x and y dimensions. To make the accuracy results comparable across different tag arrays, we reject all the RFID predictions based on partial RFID tag array readings for results in this section alone.

During the evaluation, the experimenter then moves around the tag array, while the RFID reader and antenna are placed on the floor of an empty lab space statically. The tag array is at 1 meter away from the antenna, facing the same direction and standing on the floor. We test our algorithm on six different angles relative to the antenna: 30°, 60°, 90°, 120°, 150°, 180°. We also place a Cutting Mats on the floor as the ground truth reference. For each position, we collected data for 30 seconds with three repetitions. We then try different array configurations with an aperture of 3-5 cm and a size of 6-25 (Table below).

tag array dimension	aperture (cm)	tag array size (cm^2)
2 x 3	5	7.5 x 12.5
2 x 4	5, 4	7.5 x 17.5, 6.5 x 14.5
2 x 5	4	6.5 x 18.5
3 x 3	5, 4, 3	12.5 x 12.5, 10.5 x 10.5, 8.5 x 8.5
4 x 4	5, 4, 3	17.5 x 17.5, 14.5 x 14.5, 11.5 x 11.5
5 x 5	5, 4, 3	22.5 x 22.5, 18.5 x 18.5, 14.5 x 14.5

Results: Figure 10 depicts the accuracy of different RFID tag arrays. A larger aperture leads to a higher accuracy, which can be explained by the intuition behind MUSIC algorithms (Fig. 4). The θ is calculated based on the ratio of aperture l and distance delta Δd. Increasing l makes RF-Wear algorithms more robust to the Δd measurement errors. All the tag arrays with a 5 cm spacing perform better than that with 4 cm and 3 cm spacing.

Moreover, placing more RFIDs with a small spacing also increases interference between adjacent RFIDs and reduces the accuracy as well. In all the 3cm spacing cases, the center tags are less visible than the surrounding tags. As a result, 4x4_3cm and 5x5_3cm don't produce any data. A more detailed discussion of the RFID interference can be found in Sec. 8.

Figure 10 also illustrates larger arrays produce higher accuracy results. 5x5_5cm performs better than 4x4_5cm, which works better than 3x3_5cm. While most tag arrays at 4 cm and 3 cm spacing have reasonably good accuracy,

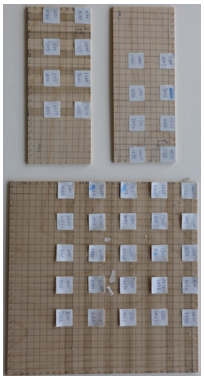

Fig. 9. Experimental wooden boards

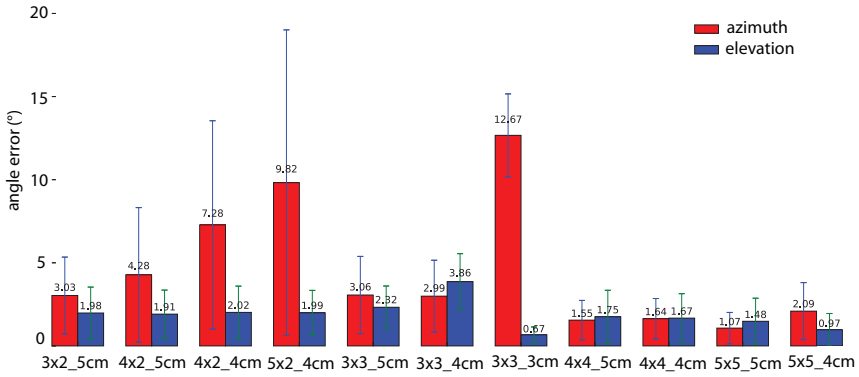

Fig. 10. Microbenchmark results. The azimuth and elevation angle measurement error for each independent tag array. *5x5_5cm* performs best while *3x3_3cm* performs worst.

the tag array choices are mainly limited by the body area. For example, small sensor arrays are suited for body parts with a smaller surface area (e.g. the upper arm), while the larger ones are best suited for larger parts (e.g. the torso or back).

Key Findings and Insights: All the tag arrays with a 5 cm spacing perform better than that with 4 cm and 3 cm spacing. This is because an increase in aperture also increases effective range of measured phases. Further, it minimizes error owing to interactions between tags. We note that larger spacing is inadvisable given that it would be larger than quarter-a-wavelength, as we discuss in Sec. 4. In effect, a choice of spacing of 5 *cm* improves system accuracy while eliminating ambiguity. In all the following experiments, we use the tag arrays with a 5 cm aperture and adjust the array dimension in accordance with the available surface area.

7.2 Fabric Flexibility

In this experiment, we evaluate the effect of fabric flexibility in the accuracy of RF-Wear.

Method: We place two rectangular arrays of 4×2 RFID tags on three clothing made of three different materials: (1) Cotton pants; (2) Wool sweater; and (3) Polyester jacket, each with varying degrees of flexibility. We place the clothing on the ground and only test our algorithm at the 90°relative to the antenna. We then intentionally create a corrugation as the one commonly seen on the body and repeat each data collection five times. The rest data collection configuration is same as Sec 7.1.

Results: Figure 11 depicts the mean and standard deviation of the error in the angle of a one-degree-of-freedom joint using RFIDs mounted on the three different types of fabric. We observe a mean error of 6.6°, 5.2° and 8.7° for a cotton, wool sweater, and polyester jacket respectively.

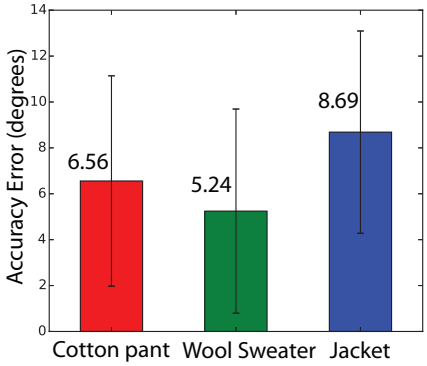

Fig. 11. **Fabric Flexibility:** We plot the broadside angle error (degrees) between the tag array and the antenna. The tag arrays were mounted on different types of fabric with intentional wrinkle: cotton pant, jean pant, wool sweater and jacket.

Key Findings and Insights: We observe that while the accuracy diminishes marginally for more flexible fabric, our system remains largely robust to the flexibility of fabric mounted on clothing owing to the algorithms described in Sec. 5.3.

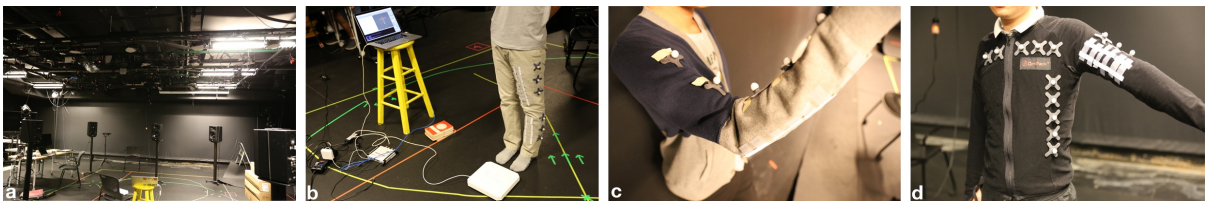

Fig. 12. **Motion Capture Apparatus**. We evaluated RF-Wear inside (5 ft)^3 space using 8 OptiTrack cameras for submillimeter 3D tracking ground-truth. The cameras are mounted on the ceiling.

7.3 Motion Capture Evaluation

In this experiment, we deploy RF-Wear on three representative joints: right elbow, left knee, and left shoulder and evaluate the angular error in a lab environment using a motion capture system. These joints represent three classes of joints in RF-Wear: 1DOF joints in upper/lower body and a 2DOF joint.

Apparatus: We conduct our evaluation in a hardware lab as depicted in Figure 12a. To emulate the reflectors in the real world, we intentionally keep the facilities in the proximity of our test position. We evaluate each joint independently and use OmniID IQ150 in all three joints. To evaluate the RF-Wear's performance with dynamic reader positions, we place an RFMAX S9028 antenna on the ground and allow the subject to move around naturally within 0.5 m from the antenna (Fig. 12b).

To obtain ground-truth joint angles during motion, we set up an 8-camera Optitrack system inside the lab space. Eight motion capture cameras are deployed on the ceiling. We affixed multiple reflector markers to different body parts (Fig. 12b, c, d) and calibrated the Optitrack to track the markers with sub-millimeter accuracy.

7.3.1 Knee Joint. **Method**: Figure 12b illustrates the evaluation configuration on the subject's left leg. Two rectangular 4×2 RFID-arrays are taped to the front side of the pants: one on the lower leg and the other on upper leg. The subject is instructed to mark time or walk around the antenna in their real life walking pose.

We then test RF-Wear in two contexts: mark time and walk around the antenna. For each context, we collect data for 60 seconds, and the subject stands still at the beginning and the ending for calibration purpose.

To retrieve the ground truth, we place six reflectors on the left side of the left legs (Fig. 12b). We reconstruct two imaginary lines (the top three and lower three reflectors respectively) using the motion capture data, and then compute the angle between these two lines. Since the angle measured from the side (motion capture) is not identical to that from the front (RF-Wear), we measure the angle different at the beginning (when the subject is still) to compute the constant offset. The offset in this subject is 22°.

We align the motion capture data with the RF-Wear predictions based on the absolute timestamps.

Results: Figure 13 plots evaluation results for the knee experiments (a, b for the mark time setting and c, d for the walk around setting).

In the mark time setting, the subject lifts his leg 17 times (counting the peaks in Fig. 13a) in 30 seconds. RF-Wear captured 1105 independent tag array readings (visualized as blue dots). The refresh rate is 36.8 Hz. We also implement a standard Kalman filter to smooth the RF-Wear predictions. Figure. 13b illustrates the angular error distribution after Kalman Filter in a CDF chart (avg = 8.89°, std = 7.73°).

In the walk around setting, the subject lifts his his leg 25 times in 40 seconds (Fig. 13c). RF-Wear captured 1585 independent tag array readings (visualized as blue dots). The refresh rate is 39.6 Hz. Figure. 13d illustrates the corresponding angular error distribution after Kalman Filter in a CDF chart (avg error = 12.50°, std = 12.52°).

Key Insights: Our system accurately tracks the angle of the joint akin to the baseline with high responsiveness, refresh rate and accuracy. When the users walk around the antenna, the system still functions correctly, although

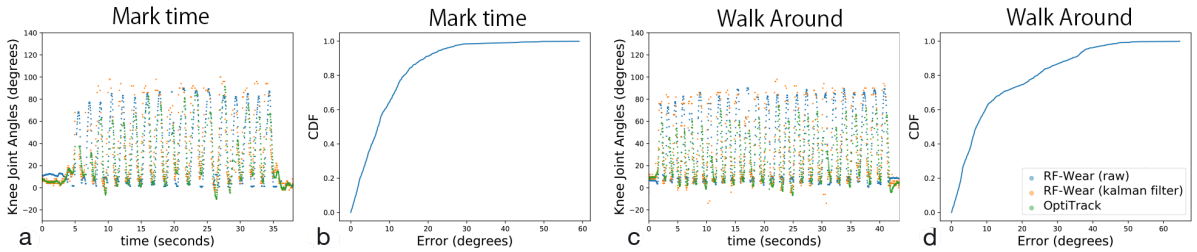

Fig. 13. **Knee results**. From left to right: a). The knee joint angle trace in the mark time setting; b). The angular error distribution plot in the mark time setting; c). The knee joint angle trace in the walk around setting; d). The angular error distribution plot in the walk around setting.

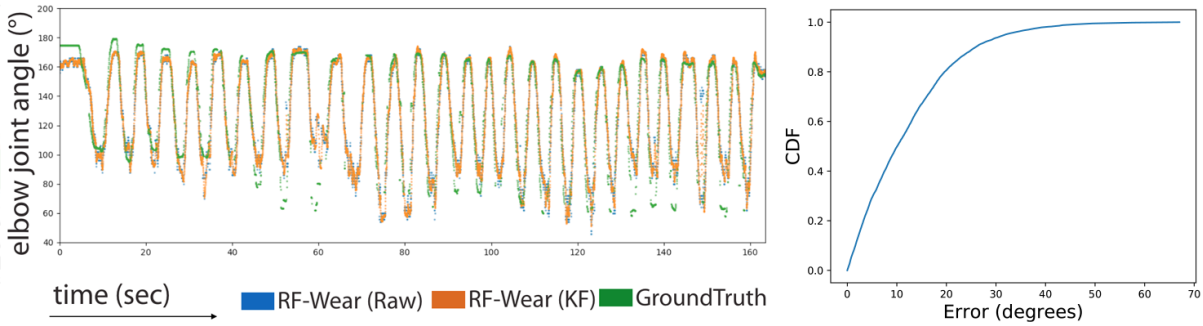

Fig. 14. **Elbow results**. Left: The elbow joint angle trace in 160 seconds data collection. Right: The angular error distribution plot for the elbow joint.

the error increases by 4°. Observe as the user walks around, the reader antenna inevitably moves over time on his body. Our system remains robust to this effect.

7.3.2 Elbow Joint. **Method**: Figure 12c illustrates the evaluation configuration on the subject's right elbow. The procedure is similar to the Knee Joint experiment. Two rectangular 4x2 RFID-arrays are taped to the bottom of the sleeve of a cotton sweater: one on the lower arm and the other on the upper arm. The subject is instructed to move the elbow as well as the shoulder to test diverse relative positions from the antenna to the tag array. We then conduct a long one-shot data collection (3 minutes) and remind the subject to change the movement pace intentionally during the evaluation.

To retrieve the ground truth, we place six reflectors on the top of the sleeve of a cotton sweater. The systematic offset in Elbow subject is 0°.

Results: Figure 14 (left) plots evaluation results for the elbow experiments. During the elbow test, the subject repeats the elbow gestures for 27 times in 155 seconds. Both the raw predictions and the Kalman Filter predictions are well aligned with the ground truth measurements from the motion capture system. Figure. 14 (right) illustrates the corresponding angular error distribution after Kalman Filter in a CDF chart (avg error = 12.31°, std = 10.19°). RF-Wear captured 11872 independent tag array readings (visualized as blue dots). The refresh rate is 76.6 Hz.

Key Insights: We observe similar high accuracy in the elbow in joint angle tracking, as with the knee. We observe a higher refresh rate in our measurements because the reader is located closer to the elbow than the knee.

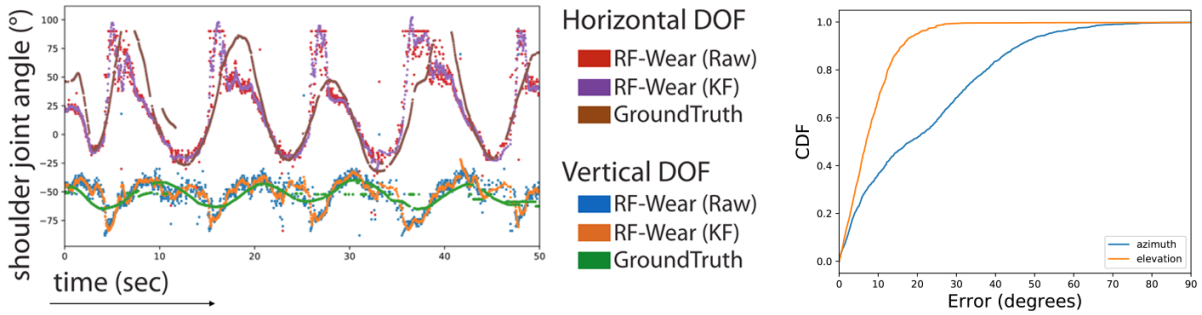

Fig. 15. **Shoulder results**. Left: The shoulder joint 2 degree of freedom angle trace. Right: The angular error distribution plot for the azimuth and elevation.

7.3.3 Shoulder Joint. **Method**: Figure 12d illustrates the evaluation configuration on the subject's left shoulder. The procedure is similar to the past two experiments. One rectangular 4x2 RFID-arrays is taped to the front of the sleeve of a cotton sweater. The subject is instructed to move the shoulder in an arbitrary path.

To retrieve the ground truth, we place ten reflectors on the chest (5 horizontally and five vertically) and three reflectors on the top of the sleeve. To compute the ground truth, we first identify the ten reflectors in the same plane and then calculate the relative azimuth/elevation angles of the arm in the plane of the chest.

Results: Figure 15 (left) illustrates the result for shoulder experiment. 1806 samples were captured in 50 seconds, with 4 peak among them. The refresh rate is 36.1Hz. Average error for azimuth and elevation angle is 21.13 °and 7.95 ° respectively, with stds 16.93° and 5.47°. Figure 15 (right) illustrates the CDF for azimuth and elevation angle after Kalman Filtering.

Key Insights: We observe a high accuracy in joint angle-tracking for two degrees of freedom. We do observe a higher error compared to the one-degree-of-freedom joints, intuitively because arrays of similar dimensions are employed to retrieve two independent angles. Note that the error in polar angle is lower than the azimuth, because the polar angle can at its highest be 90 degrees while the azimuthal angle varies between 0 and 360 degrees.

8 DISCUSSION AND LIMITATIONS

8.1 Advantages and Limitations of RFIDs for smart fabrics

Using passive tags for body-frame tracking has two key advantages. First, passive RFID tags harvest energy off the radio waves from the reader antenna, and do not require batteries or complex circuits on the clothes. Clothes, which require daily maintenance, will remain machine washable. Second, wireless RFID networks are programmable. RF-Wear's approach can turn regular clothes into smart suits by weaving RFIDs into fabric. A few important limitations of our choice of RFIDs for smart-fabrics: First, we assume the presence of a reader which is in range (few meters) of the tags (e.g. in the user's pocket or a desk nearby). Second, the reader needs to be recharged much like a smartphone. However, the increasing proliferation of RFIDs and the potential of future smartphones to have RFID reader chips [18] bolsters the deployability and applicability of RF-Wear.

8.2 Tracking clothes vs. the body

RF-Wear tracks the body-frame by tracking the way clothes move as the body moves. This imposes a limitation: RF-Wear can only track the joints covered by clothing. Besides, RF-Wear also does not track angles at extremities

such as the fingers and toes, given that they offer too small a surface area to attach a RFID array. The joints supported by RF-Wear are the elbow, shoulder, neck, hip, and knees.

In our experiments, we find that there are two unique types of movements of clothing: skeletal movement (e.g. changing the elbow joint angle) and frictional movement (e.g. rotation of the waist). This paper mainly explores skeletal movement in body-frame tracking. Frictional movement occurs due to various factors beyond the body movement, e.g. the tightness of the clothes and the material friction. A possible approach to measure friction movement is to place additional RFID tags directly on the skin as tattoos [41]. A study of this, however, is beyond the scope of this paper.

8.3 Increasing number of RFID Tags vs. Refresh Rate

Our current prototype requires two 4x2 tag arrays to track each joint and six 4x2 tag arrays on the body resulting 24x4 (knees, elbows, hips, shoulders) + 8x6 (main body) = 144 tags in total. Since some of the tags can be reused in different joints (e.g. upper arm part can be used for both the shoulder and elbow), the minimum number of required tags is 112 (64 on four limbs + 48 on the main body) tags to track all the joints described above. Improved performance can result from redundant tags to avoid noise and body occlusion at special angles, e.g. by placing tags on the chest as well as the back.

While mounting a larger number of RFID tags would improve accuracy and robustness, one would need to consider whether the reader can query all tags in real-time from a single hand-held reader. Specifically, any increase in the number of tags will be bottlenecked by the reader's processing capability (2200 readings/s), reducing the refresh rate per tag [17]. In our evaluation, the refresh rate for each tag decreases steadily as the number of tags increases (50 Hz for 8 tags to 16 tags for 30 Hz).

8.4 RFID interactions: with human body and between themselves

The human body attenuates RF signals and can distort the radiation pattern and affect the antenna efficiency of RFIDs. These issues are akin to RFID tags atop metal objects whose presence strongly affects dipole antenna based RFID tags [30]. We therefore choose metal friendly RFID tags in RF-Wear and find they also work well on the body. Two important challenges stem from the occlusion of RF signals by the human body. The first is multipath ambiguity as described in Sec. 4.3, which we explicitly deal with. Second is the fact that a small number of RFID tags furthest away from the reader may be out-of-range due to excessive shadowing. Adding extra tags at different orientations on the fabric or using improved or special RFID tags designed for the body can potentially remedy this situation. Indeed designing RFID tag array configurations that suit different body types, types of clothing, can be sewn into fabric and have sufficient redundancy is an important engineering problem.

One might wonder if the phase of RFID tags are affected significantly by the presence of others. Our experiments space adjacent RFID tags at a relative distance of 2.5 *cm* or higher, resulting in empirically observed phase error (i.e. difference in phase with and without an adjacent tag) of at most 10°. Overall these interferences impacts accuracy negligibly when compared to other measurement noise (e.g. tag orientations).

8.5 Data-Driven solutions that incorporate body-kinematics

RF-Wear's accuracy can be greatly improved by incorporating body kinematics, data pertaining to human movement and even learning patterns of movement of a given user. Our current approach intentionally does not calibrate to specific users to present native accuracy from RFID-tracking. However, future systems can employ algorithms such as the random forest decision tree [37] to account for body kinematics and filter observed data.

8.6 Power consumption

The RFID reader used in our prototype supports four antennas and consumes more power than RF-Wear requires. A comparable COTS reader can be ThingMagic Micro [40]. This two-antenna-port reader can process 750 tag readings/s and will consume $3w$ during scanning and $0.06w$ during idle. These numbers are comparable to the widely deployed Wi-Fi cards (active: $2w$; idle: $1w$ [6]). A further hardware customization can further bring down the cost and improve the power efficiency.

9 CONCLUSION AND FUTURE WORK

This paper presents RF-Wear, an accurate and wearable system to track a user's body frame using low-cost passive RFIDs embedded in their clothing. RF-Wear achieves this by processing wireless signals reflected off these tags to a compact single-antenna RFID reader. In doing so, RF-Wear enables a first-of-its-kind body-frame tracking system that is lightweight and convenient for everyday use, without the need for external infrastructure. We implement and evaluate a prototype of RF-Wear on commercial RFID readers and tags and demonstrate its performance in body-frame tracking. We believe RF-Wear will form a key primitive for a variety of applications in gesture-based interfaces, health monitoring and fitness tracking. While RF-Wear tracks the angle of joints on the body in 3-D, it cannot track more fine-grained changes in curvature of the body, e.g. due to curvature of the spine. We believe this is an important area for future investigation.

REFERENCES

[1] 2017. TSL 1153 Bluetooth UHF RFID Reader. https://www.atlasrfidstore.com/tsl-1153-bluetooth-uhf-rfid-reader/. (2017). (Accessed on 05/15/2017).

[2] Fadel Adib, Zachary Kabelac, Dina Katabi, and Robert C Miller. 3D Tracking via Body Radio Reflections.

[3] Eric R Bachmann, I Duman, UY Usta, Robert B McGhee, XP Yun, and MJ Zyda. 1999. Orientation tracking for humans and robots using inertial sensors. In *Computational Intelligence in Robotics and Automation, 1999. CIRA'99. Proceedings. 1999 IEEE International Symposium on*. IEEE, 187–194.

[4] Alan Bränzel, Christian Holz, Daniel Hoffmann, Dominik Schmidt, Marius Knaust, Patrick Lühne, René Meusel, Stephan Richter, and Patrick Baudisch. 2013. GravitySpace: tracking users and their poses in a smart room using a pressure-sensing floor. In *Proceedings of the SIGCHI Conference on Human Factors in Computing Systems*. ACM, 725–734.

[5] Ke-Yu Chen, Kent Lyons, Sean White, and Shwetak Patel. 2013. uTrack: 3D input using two magnetic sensors. In *Proceedings of the 26th annual ACM symposium on User interface software and technology*. ACM, 237–244.

[6] Salvatore Chiaravalloti, Filip Idzikowski, and Lukasz Budzisz. 2011. Power consumption of WLAN network elements. *Tech. Univ. Berlin, Tech. Rep. TKN-11-002* (2011).

[7] P Daponte, J De Marco, L De Vito, B Pavic, and S Zolli. 2011. Electronic measurements in rehabilitation. In *Medical Measurements and Applications Proceedings (MeMeA), 2011 IEEE International Workshop on*. IEEE, 274–279.

[8] Artem Dementyev, Hsin-Liu Cindy Kao, and Joseph A Paradiso. 2015. Sensortape: Modular and programmable 3d-aware dense sensor network on a tape. In *Proceedings of the 28th Annual ACM Symposium on User Interface Software & Technology*. ACM, 649–658.

[9] Han Ding, Longfei Shangguan, Zheng Yang, Jinsong Han, Zimu Zhou, Panlong Yang, Wei Xi, and Jizhong Zhao. 2015. Femo: A platform for free-weight exercise monitoring with rfids. In *Proceedings of the 13th ACM Conference on Embedded Networked Sensor Systems*. ACM, 141–154.

[10] Jonny Farringdon, Andrew J Moore, Nancy Tilbury, James Church, and Pieter D Biemond. 1999. Wearable sensor badge and sensor jacket for context awareness. In *Wearable Computers, 1999. Digest of Papers. The Third International Symposium on*. IEEE, 107–113.

[11] Brian P Flanagan and Kristine L Bell. 2001. Array self-calibration with large sensor position errors. *Signal Processing* 81, 10 (2001), 2201–2214.

[12] Sean Follmer, Daniel Leithinger, Alex Olwal, Nadia Cheng, and Hiroshi Ishii. 2012. Jamming user interfaces: programmable particle stiffness and sensing for malleable and shape-changing devices. In *Proceedings of the 25th annual ACM symposium on User interface software and technology*. ACM, 519–528.

[13] B Gupta, S Sankaralingam, and S Dhar. 2010. Development of wearable and implantable antennas in the last decade: A review. In *Microwave Symposium (MMS), 2010 Mediterranean*. IEEE, 251–267.

[14] John Hewitt. 2013. The MYO Gesture-Control Armband Sense Your Muscle's Movements, ExtremeTech (online magazine), Feb. 27. (2013).

[15] Tran Nhat Hung and Young Soo Suh. 2013. Inertial sensor-based two feet motion tracking for gait analysis. *Sensors* 13, 5 (2013), 5614–5629.
[16] Takeo Igarashi and John F Hughes. 2006. Clothing manipulation. In *ACM SIGGRAPH 2006 Courses*. ACM, 21.
[17] Impinj Inc. 2017. Speedway Reader R420. https://www.impinj.com/platform/connectivity/speedway-r420/. (2017).
[18] RFID Insider. 2014. RFID Readers For Mobile Phones From TSL. http://blog.atlasrfidstore.com/rfid-readers-mobile-phones-tsl. (2014).
[19] Tiiti Kellomäki, Johanna Virkki, Sari Merilampi, and Leena Ukkonen. 2012. Towards washable wearable antennas: a comparison of coating materials for screen-printed textile-based UHF RFID tags. *International Journal of Antennas and Propagation* 2012 (2012).
[20] Goojo Kim, Jinseong Lee, Kyoung Hwan Lee, You Chung Chung, Junho Yeo, Byung Hyun Moon, Jeenmo Yang, and Hee Cheol Kim. 2008. Design of a UHF RFID fiber tag antenna with electric-thread using a sewing machine. In *Microwave Conference, 2008. APMC 2008. Asia-Pacific*. IEEE, 1–4.
[21] Yeonho Kim, Kyounghwan Lee, Yongju Kim, and You Chung Chung. 2007. Wearable UHF RFID tag antenna design using flexible electro-thread and textile. In *Antennas and Propagation Society International Symposium, 2007 IEEE*. IEEE, 5487–5490.
[22] Hanchuan Li, Can Ye, and Alanson P Sample. 2015. IDSense: A human object interaction detection system based on passive UHF RFID. In *Proceedings of the 33rd Annual ACM Conference on Human Factors in Computing Systems*. ACM, 2555–2564.
[23] Hanchuan Li, Peijin Zhang, Samer Al Moubayed, Shwetak N Patel, and Alanson P Sample. 2016. Id-match: A hybrid computer vision and rfid system for recognizing individuals in groups. In *Proceedings of the 2016 CHI Conference on Human Factors in Computing Systems*. ACM, 4933–4944.
[24] Tianxing Li, Chuankai An, Zhao Tian, Andrew T Campbell, and Xia Zhou. 2015. Human sensing using visible light communication. In *Proceedings of the 21st Annual International Conference on Mobile Computing and Networking*. ACM, 331–344.
[25] Thomas B Moeslund and Erik Granum. 2001. A survey of computer vision-based human motion capture. *Computer vision and image understanding* 81, 3 (2001), 231–268.
[26] Leap Motion. 2015. Leap motion controller. *URl: https://www. leapmotion. com* (2015).
[27] Gauri Nanda, Adrian Cable, V Michael Bove, Moneta Ho, and Han Hoang. 2004. bYOB [Build Your Own Bag]: a computationally-enhanced modular textile system. In *Proceedings of the 3rd international conference on Mobile and ubiquitous multimedia*. ACM, 1–4.
[28] Lionel M Ni, Yunhao Liu, Yiu Cho Lau, and Abhishek P Patil. 2004. LANDMARC: indoor location sensing using active RFID. *Wireless networks* 10, 6 (2004), 701–710.
[29] Pavel V Nikitin and KV Seshagiri Rao. 2010. Compact Yagi antenna for handheld UHF RFID reader. In *Antennas and Propagation Society International Symposium (APSURSI), 2010 IEEE*. IEEE, 1–4.
[30] Cecilia Occhiuzzi, Stefano Cippitelli, and Gaetano Marrocco. 2010. Modeling, design and experimentation of wearable RFID sensor tag. *IEEE Transactions on Antennas and Propagation* 58, 8 (2010), 2490–2498.
[31] Ryo Ohsawa, Masayuki Iwai, Takuya Imaeda, Kei Suzuki, Takuro Yonezawa, Kazunori Takashio, and Hideyuki Tokuda. 2006. Smartfuroshiki: A sensorized fabrics supporting office activities. In *UbiComp'06: Proceedings of the 8th International Conference on Ubiquitous Computing*, Vol. 9.
[32] Natural Point. 2011. Optitrack. *Natural Point, Inc.,[Online]. Available: http://www. naturalpoint. com/optitrack/.[Accessed 22 2 2014]* (2011).
[33] Ivan Poupyrev, Nan-Wei Gong, Shiho Fukuhara, Mustafa Emre Karagozler, Carsten Schwesig, and Karen E Robinson. 2016. Project Jacquard: Interactive Digital Textiles at Scale. In *Proceedings of the 2016 CHI Conference on Human Factors in Computing Systems*. ACM, 4216–4227.
[34] Qifan Pu, Sidhant Gupta, Shyamnath Gollakota, and Shwetak Patel. 2013. Whole-home gesture recognition using wireless signals. In *Proceedings of the 19th annual international conference on Mobile computing & networking*. ACM, 27–38.
[35] Damien Rohmer, Tiberiu Popa, Marie-Paule Cani, Stefanie Hahmann, and Alla Sheffer. 2010. Animation wrinkling: augmenting coarse cloth simulations with realistic-looking wrinkles. In *ACM Transactions on Graphics (TOG)*, Vol. 29. ACM, 157.
[36] Ralph Schmidt. 1986. Multiple emitter location and signal parameter estimation. *IEEE transactions on antennas and propagation* 34, 3 (1986), 276–280.
[37] Jamie Shotton, Toby Sharp, Alex Kipman, Andrew Fitzgibbon, Mark Finocchio, Andrew Blake, Mat Cook, and Richard Moore. 2013. Real-time human pose recognition in parts from single depth images. *Commun. ACM* 56, 1 (2013), 116–124.
[38] Tien-Wei Shyr, Jing-Wen Shie, Chang-Han Jiang, and Jung-Jen Li. 2014. A textile-based wearable sensing device designed for monitoring the flexion angle of elbow and knee movements. *Sensors* 14, 3 (2014), 4050–4059.
[39] Andrew Spielberg, Alanson Sample, Scott E Hudson, Jennifer Mankoff, and James McCann. 2016. RapID: A framework for fabricating low-latency interactive objects with RFID tags. In *Proceedings of the 2016 CHI Conference on Human Factors in Computing Systems*. ACM, 5897–5908.
[40] ThingMagic. 2017. ThingMagic M6E Family: Performance, Efficiency and Flexibility - Tech Spec Sheets. (2017). (Accessed on 10/16/2017).
[41] James Tribe, Dumtoochukwu Oyeka, John Batchelor, Navjot Kaur, Diana Segura-Velandia, Andrew West, Robert Kay, Katia Vega, and Will Whittow. 2015. Tattoo antenna temporary transfers operating on-skin (TATTOOS). In *International Conference of Design, User Experience, and Usability*. Springer, 685–695.

[42] Leena Ukkonen, Lauri Sydänheimo, and Markku Kivikoski. 2007. Read range performance comparison of compact reader antennas for a handheld UHF RFID reader. In *RFID, 2007. IEEE International Conference on*. IEEE, 63–70.
[43] Jue Wang, Deepak Vasisht, and Dina Katabi. 2015. RF-IDraw: virtual touch screen in the air using RF signals. *ACM SIGCOMM Computer Communication Review* 44, 4 (2015), 235–246.
[44] Shiqi Wang, Ngai Lok Chong, Johanna Virkki, Toni Björninen, Lauri Sydänheimo, and Leena Ukkonen. 2015. Towards washable electrotextile UHF RFID tags: Reliability study of epoxy-coated copper fabric antennas. *International Journal of Antennas and Propagation* 2015 (2015).
[45] Roy Want. 2006. An introduction to RFID technology. *IEEE pervasive computing* 5, 1 (2006), 25–33.
[46] Teng Wei and Xinyu Zhang. 2016. Gyro in the air: tracking 3D orientation of batteryless internet-of-things. In *Proceedings of the 22nd Annual International Conference on Mobile Computing and Networking*. ACM, 55–68.
[47] Jie Xiong and Kyle Jamieson. 2013. ArrayTrack: A Fine-Grained Indoor Location System.. In *NSDI*. 71–84.
[48] Lei Yang, Yekui Chen, Xiang-Yang Li, Chaowei Xiao, Mo Li, and Yunhao Liu. 2014. Tagoram: Real-time tracking of mobile RFID tags to high precision using COTS devices. In *Proceedings of the 20th annual international conference on Mobile computing and networking*. ACM, 237–248.
[49] Lining Yao, Jifei Ou, Chin-Yi Cheng, Helene Steiner, Wen Wang, Guanyun Wang, and Hiroshi Ishii. 2015. BioLogic: natto cells as nanoactuators for shape changing interfaces. In *Proceedings of the 33rd Annual ACM Conference on Human Factors in Computing Systems*. ACM, 1–10.
[50] Yang Zhang, Junhan Zhou, Gierad Laput, and Chris Harrison. 2016. Skintrack: Using the body as an electrical waveguide for continuous finger tracking on the skin. In *Proceedings of the 2016 CHI Conference on Human Factors in Computing Systems*. ACM, 1491–1503.
[51] Zhengyou Zhang. 2012. Microsoft kinect sensor and its effect. *IEEE multimedia* 19, 2 (2012), 4–10.

Received May 2017; Revised Aug 2017; Accepted Oct 2017